SYSTEM DESIGN AND SIGNAL PROCESSING METHOD FOR TRACKING ULTRASONIC RANGING

Xuewu QIAN[1,2]

The widespread use of ultrasonic ranging can be attributed to its low cost, high measurement accuracy and ease of use. However, the accuracy of ultrasonic ranging is significantly affected by environmental factors, necessitating comprehensive investigation. This paper presents an analysis of the principle of tracking ultrasonic ranging, a description of the circuit design and timing logic, and a proposal for a combined filtering algorithm combining median filtering with Kalman filtering. The results of the testing demonstrate that the combined filtering method has the potential to significantly enhance the accuracy and stability of the measurements. In the range of 3 metres, the measurement error can reach ±1 mm. In comparison with traditional methods, the level of precision achieved is 50% greater, which lends considerable weight to the potential applicability of this methodology.

Keywords: Ultrasonic ranging, Tracking type, Median filtering, Kalman filtering

1. Introduction

At present, the predominant ranging techniques employ laser, infrared, camera systems, ultrasonic, and other ranging technologies. The operational principles of different ranging technologies vary. Ultrasonic technology is frequently employed for distance measurement due to its high degree of directivity, low energy loss, cost-effectiveness, and extended propagation range within the medium [1-3]. Ultrasonic vibrations in the air can be generated and measured by ultrasonic sensors. In industrial automation, ultrasonic sensors are commonly used to measure the distance and position of objects, monitor the position of objects or robots on production lines, control the movement of robots, detect the presence of objects, or measure liquid levels; with the development of AI, ultrasonic sensors are also widely used in vehicles and robots to detect obstacles in the surroundings and to enhance the recognition ability of AI .

The methods of ultrasonic ranging developed by scholars both domestically and internationally can be broadly classified into three main categories: the time-of-flight method, the phase difference detection method, and

[1] Prof., Department of Electronic Engineering, Jinan Vocational College, Jinan 250103, China, e-mail: sdqxwu@163.com
[2] Jinan Key Laboratory of 5G + Advanced Control Technology, Jinan Vocational College, Jinan 250103, China.

the multi-frequency ranging method [4-6]. Despite certain inherent limitations, the time-of-flight method is widely employed in non-high-precision distance measurement due to its relatively simple structure, convenient testing procedures, and low cost [7-8]. In this paper, the time-of-flight method is adopted to achieve distance measurement.

The fundamental principle underlying the time-of-flight method for ranging is analogous to that of radar ranging. The method entails measuring the flight time of ultrasonic waves between the ultrasonic transmitting probe and the ultrasonic receiving probe. This paper primarily presents the fundamental principles of ultrasonic ranging, circuit design, and data processing methods. In order to enhance the precision of the measurements, a combination filtering algorithm, which utilises both median filtering and Kalman filtering, is employed for the estimation of distances. The results of the experimental testing demonstrate that this method can effectively enhance the precision of the measurements taken. Furthermore, it has been established that this approach has significant implications for guiding and enhancing the stability of the measurements obtained. It has a large application prospect in two-vehicle and multi-vehicle tracking, collision avoidance or coordinated control between robots.

2. Working principle for tracking ultrasonic ranging

The tracking ultrasonic ranging system comprises a transmitter and a receiver, or alternatively, a transmitter and multiple receivers. The transmitter is primarily composed of an ultrasonic transmitting probe and an infrared emitting tube, while the receiver is primarily composed of an ultrasonic receiving probe and an infrared receiving tube. This paper primarily presents a tracking ultrasonic ranging system comprising a transmitter and a receiver, as illustrated in Fig. 1.

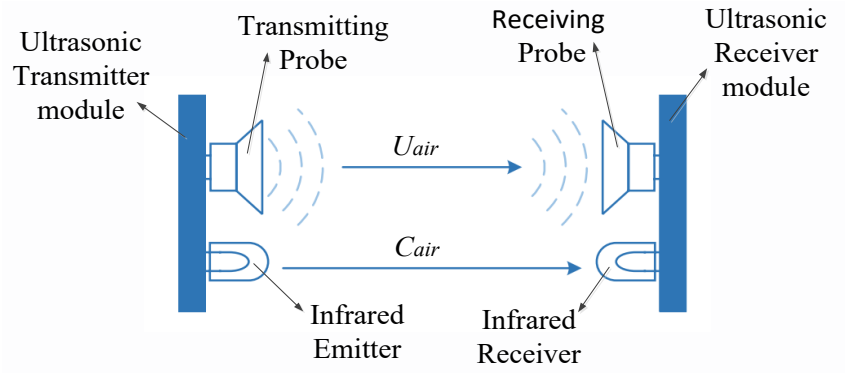

Fig. 1. Schematic diagram for tracking ultrasonic ranging

The basic process of tracking ultrasonic ranging is as follows: firstly, the ultrasonic transmitting module sends a trigger signal to the infrared transmitting tube and the ultrasonic transmitting probe at the same time, because the speed of the infrared signal is close to the speed of light, and it can be regarded as an instantaneous completion of the action, and then the infrared receiving head of the ultrasonic receiving module receives the infrared signal and starts timing, and after a period of time t, finally, the ultrasonic receiving probe of the ultrasonic receiving module receives the ultrasonic signal stops timing, then this time t is the time of ultrasonic wave propagation. The distance between the transmitter and the receiver can be calculated using the following formula:

$$s=U_{air}\cdot t \tag{1}$$

where U_{air} is the speed of sound in the air (≈ 343.2 m/s).

Assuming a maximum ranging distance of 5 meters, the maximum ultrasonic ranging error caused by infrared pulse synchronisation can be calculated as follows:

$$\Delta s=\frac{5}{C_{air}}\cdot U_{air}\approx 0.0057mm<0.01mm \tag{2}$$

where Δs is the distance error; C_{air} is the speed of light in the air (≈ 299792458 m/s). From the formula (1), it can be observed that the ranging error resulting from the utilisation of the speed of light as the synchronisation signal is less than 0.01mm, which can be deemed insignificant in the context of general distance measurement. It can therefore be posited that the transmitting and receiving modules operate in unison, and that infrared light may be employed as a synchronisation signal in theory.

3. Circuit system design and trigger signal analysis

The ultrasonic probe model is designated TCT40-16. Its centre frequency is 40 kHz, and its transmit sound pressure power exceeds 117 dB, while its receiving sensitivity exceeds -65 dB. The ultrasonic receiving chip employs the CX20106A, the infrared receiving tube utilises the IRM-3640T, and the infrared emitting tube with a wavelength of 940nm is employed as the synchronisation signal. The Hongjing Technology microcontroller (STC8G1K08) serves as the primary control unit, tasked with the reception and data processing of ultrasonic signals.

A schematic diagram of the transmitter module is provided in Fig. 2 for reference. The P3.2 port of the microcontroller serves the dual purpose of

controlling both the infrared emitter and the ultrasonic transmitting probe, thereby ensuring signal synchronisation and optimal ultrasonic output.

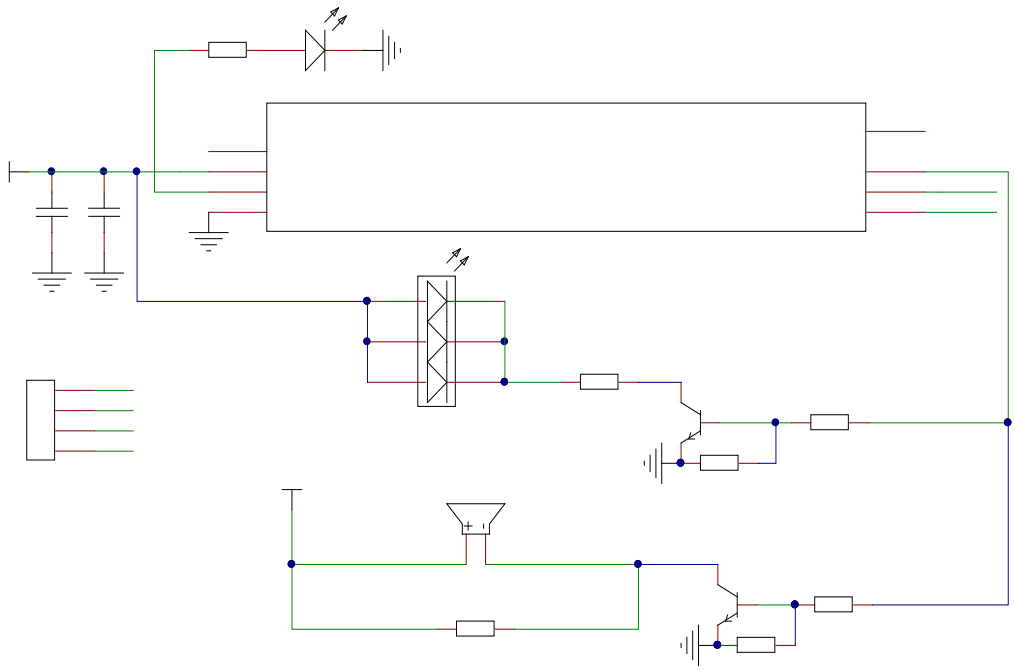

Fig. 2. Schematic Diagram of the Transmitter Module

A schematic diagram of the receiver module is provided in Fig. 3 for reference. The P3.3 port of the microcontroller is linked to the output terminal of the infrared receiver tube, while the P3.2 port is connected to pin 7 of the CX20106A. Upon the detection of a valid ultrasonic wave, the pin 7 of the CX20106A device generates a low-level signal.

The processor on the transmitter module simultaneously transmits an 8-cycle modulated signal at a frequency of 40 kHz to the transmitter probe and the infrared emitter. Since infrared light travels near the speed of light, the infrared receiver tube on the receiver module immediately generates a falling edge pulse signal. Subsequently, after a time of Δt , the ultrasonic receiver probe on the receiver module picks up the ultrasonic signal and outputs a falling edge pulse signal. By calculating the time interval between the two falling edges, the distance between the transmitter and receiver modules can be determined.

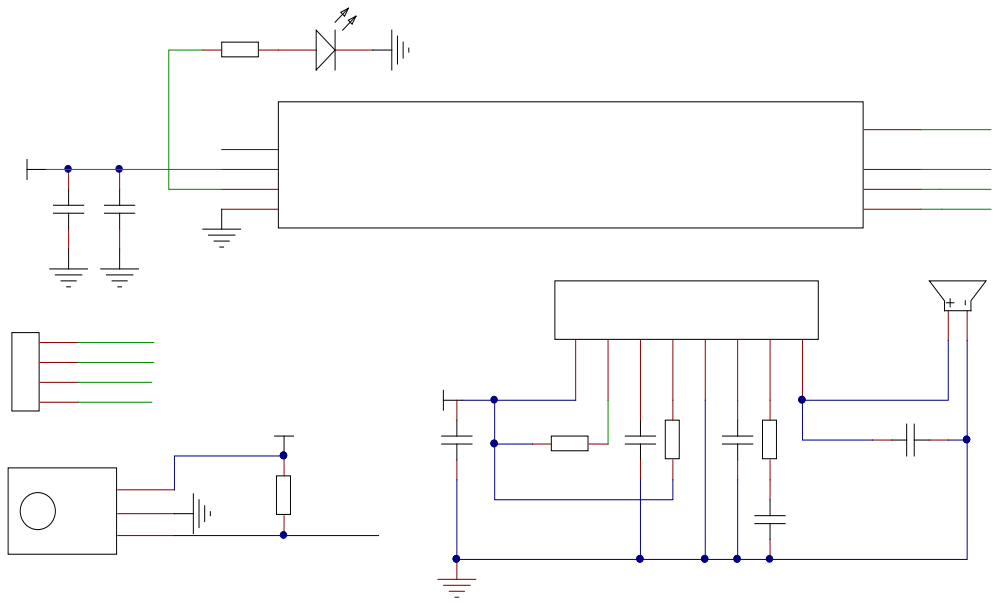

Fig. 3. Schematic Diagram of the Receiver Module

The timing logic diagram is shown in Fig. 4. As shown in Fig. 4, the distance between the transmitter and receiver modules can be calculated by accurately determining the time interval Δt, using the formula (1).

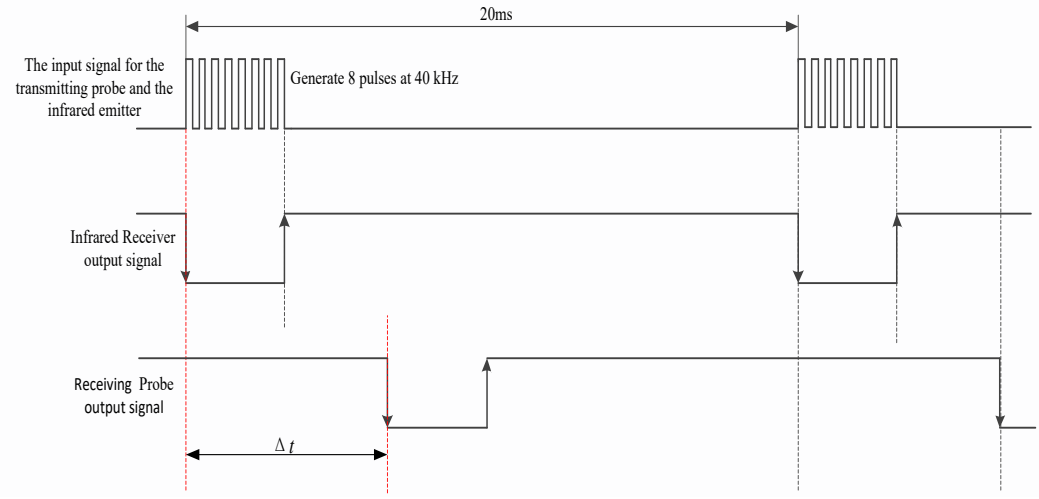

Fig. 4. Timing Logic Diagram of Trigger Signal

4. Data collection and processing method

Set the mode of microcontroller timer 1 on the receiver module to interrupt with a timing period of 20 ms. In addition, configure ports P3.2 and P3.3 as falling edge interrupts. Timer 2 will start as soon as a falling edge is detected on port P3.3. Conversely, once a falling edge is detected on P3.2, Timer 2 should stop and read the count value from the timer register. The resulting value is then multiplied by the smallest counting unit (in this case 1us) to get the time Δt,, which is then multiplied by the speed of sound to get the distance. Finally, the distance data is output through the serial port.

After testing, it was found that there were several interfering data that affected the measurement accuracy. Therefore, it was necessary to preprocess the data. In order to effectively filter out the interference, a median filtering algorithm was proposed (This article presents an improvement to the median filtering method, where 5 data points are collected and then arranged in descending order. The third data point is taken as the true value. Tests have shown that this method effectively filters out anomalous interference data.), and then Kalman filtering was used to filter the processed data. The specific implementation steps are as follows:

Step 1: Collect 5 data points and arrange them in ascending order.

Step 2: Extract the 3th data point as valid data and save it to an array.

Step 3: Implement real-time Kalman filtering on the data obtained in Step 2, and save the filtered data. The five formulas utilized in Kalman filtering are as follows [9]:

$$\begin{cases} \hat{x}(k \mid k-1) = Ax(k-1 \mid k-1) \\ P(k \mid k-1) = AP(k-1 \mid k-1)A^T + Q(k) \\ K(k \mid k-1) = P(k \mid k-1)H^T[R(k) + HP(k \mid k-1)H^T]^{-1} \\ \hat{x}(k) = \hat{x}(k \mid k-1) + K(k)[Y(k) - H\hat{x}(k \mid k-1)] \\ P(k \mid k) = [I - K(k)H]P(k \mid k-1) \end{cases} \tag{3}$$

Step 4: Output and display the distance information.

Step 5: Collect and update the data, and perform real-time recursion on the updated data.

The specific flowchart of the combined filtering algorithm is shown in Fig.5.

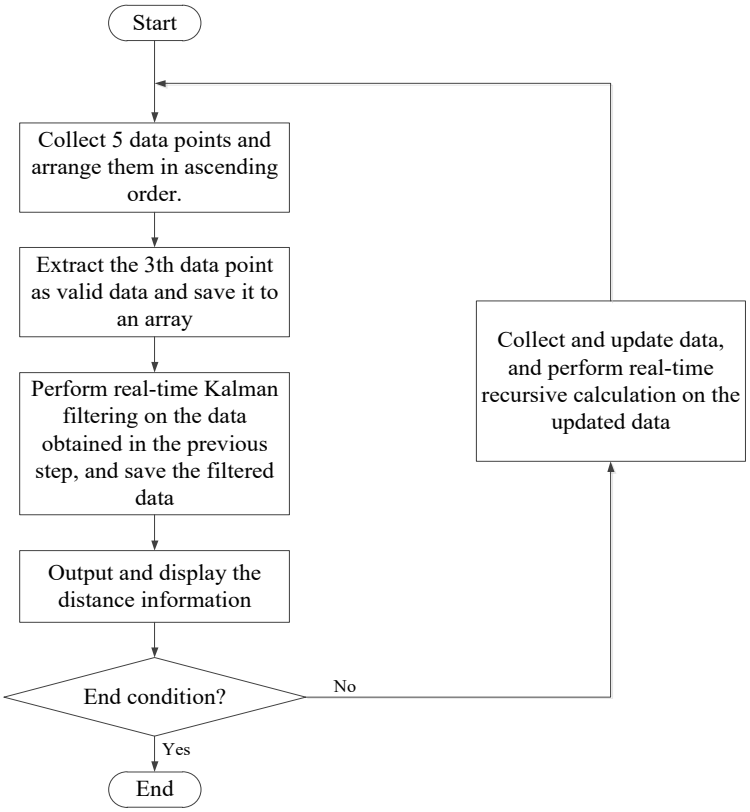

Fig. 5. Flow chart of the combined filtering algorithm

5. Implementation and verrification

The accuracy of ultrasonic ranging is susceptible to fluctuations due to external factors such as temperature and airflow. As the distance between the transmitting and receiving devices increases, the accuracy of the measurement is likely to decline. In this test, a comparison is made between the raw data, median filtering, and combined filtering for the collected data at a distance of 5 metres, as illustrated in Fig. 6.

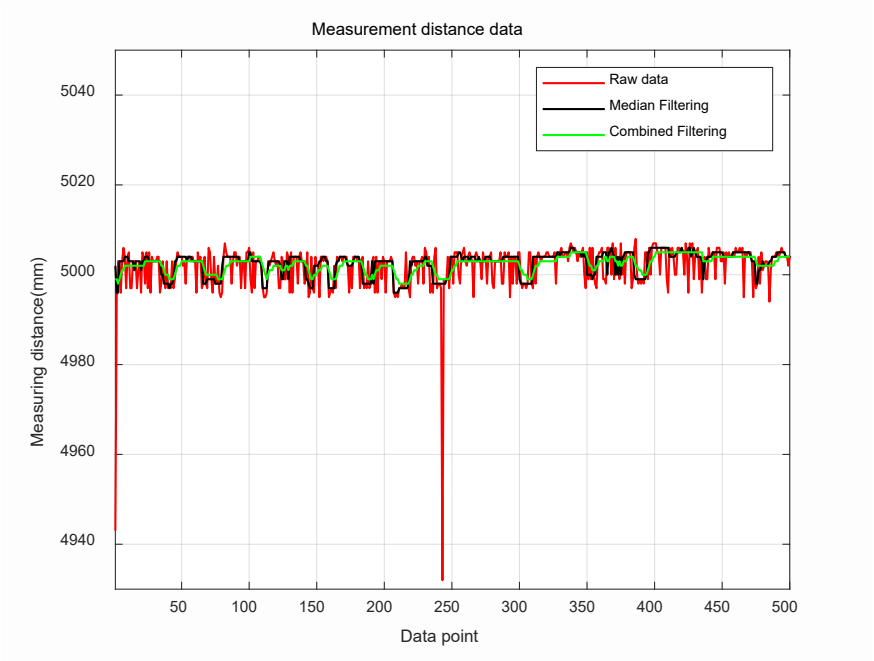

Fig. 6. Comparison of Filtering Methods at a Distance of 5 Meters

As shown in Fig. 6, there is interference data in the original data. The median filtering algorithm can effectively remove the interference data, but there are still large fluctuations; and the combined filtering method can further improve the measurement accuracy, thus realising high-precision distance measurement.

The distances between the fixed receiver and the transmitter were set as 0.2 m, 0.5 m, 1.5 m, 2 m, 3 m and 5 m. The data were processed using the median filter and Kalman filter. The data processing method adopts the median filter and Kalman filter combined filtering algorithm. The test site is shown in Fig. 7. As can be seen in Fig. 7, the ultrasonic distance measurement system consists of an ultrasonic transmitter test board, an ultrasonic receiver test board, a wireless transceiver, and a laser rangefinder; wherein the ultrasonic transmitter test board places an ultrasonic transmitter module, the ultrasonic receiver test board places an ultrasonic receiver module, and also has wireless transceiver functionality for transmitting the distance data, and the wireless transceiver is used to receive the distance data sent by the ultrasonic receiver. The wireless transceiver is used to receive the distance data sent by the ultrasonic receiver and send the received data to the computer through the serial port, and the computer's upper computer software receives the distance data and saves it, and the interface of the distance data received by the serial port is shown in Fig. 8. The laser rangefinder is used to calibrate the ultrasonic distance.

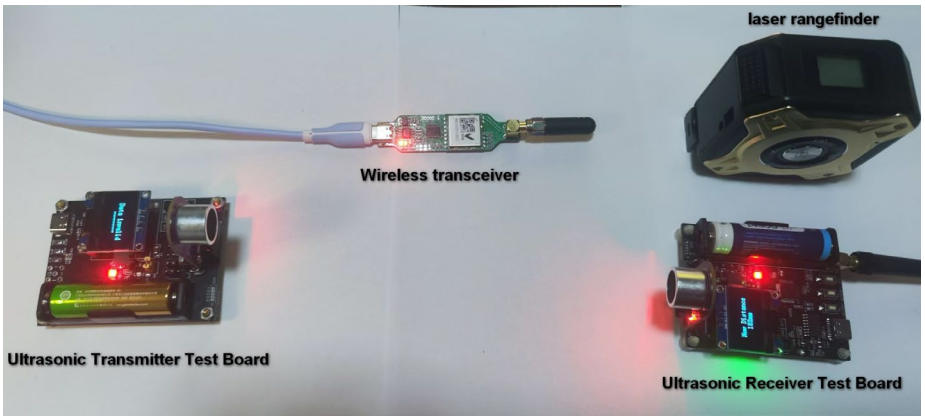

Fig. 7. The Experimental Test Site

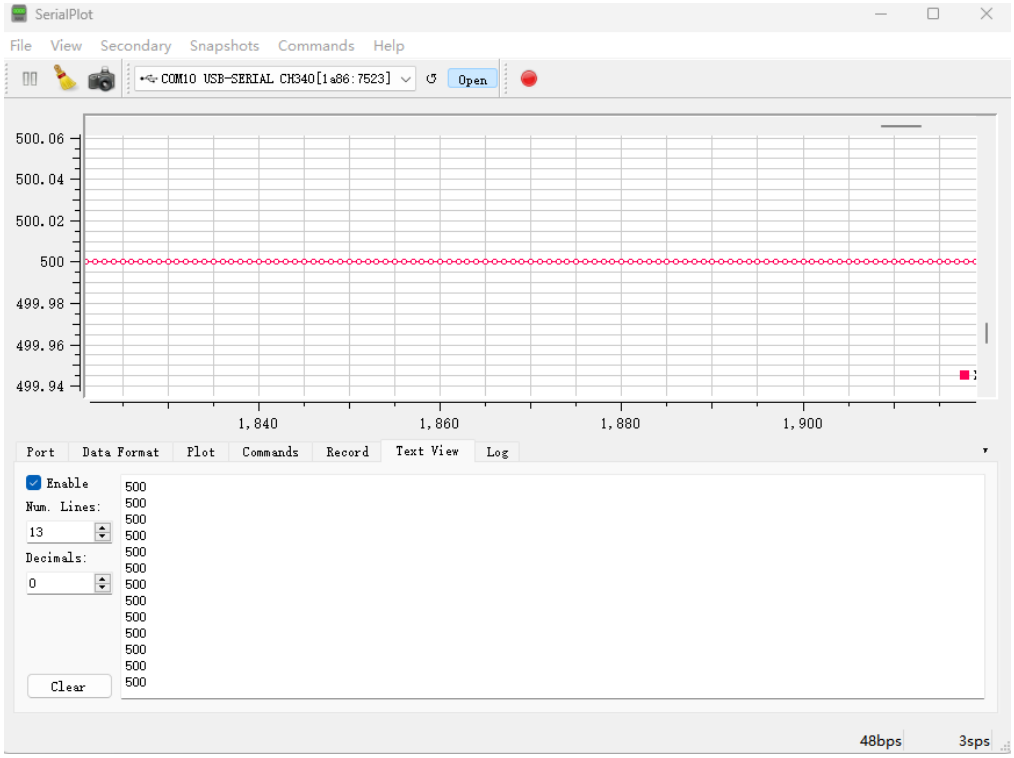

Fig. 8. Serial Data Receiving Interface

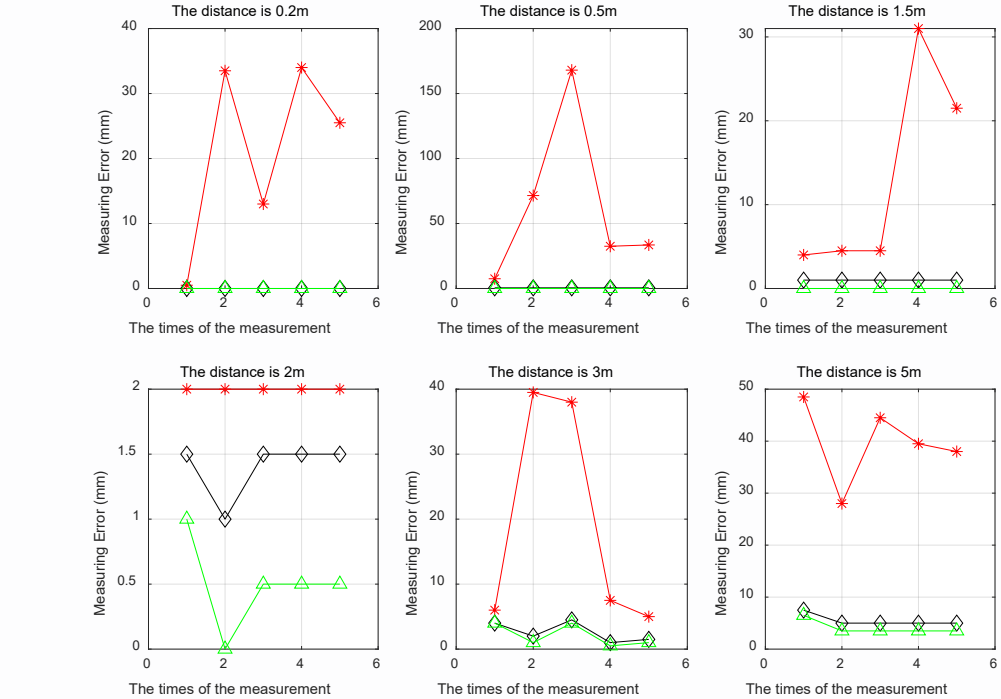

Fig. 9. Measurement Stability

Fig. 9 shows the maximum ranging error when fixing the six distance points. Five measurements were taken at each fixed point and 500 data points were collected each time. Subsequently, the maximum data fluctuation for each data set was determined as the measurement error. The distance measurement error was calculated using the following formula:

$$DataErr[i] = \left(\max_{j=1}^{500}[A_{ij}] - \min_{j=1}^{500}[A_{ij}] \right) \Big/ 2 \tag{4}$$

In the formula, A_{ij} represents a set of data measured each time, where i is the index of each set and j is the index of the data.

The measurement error is dependent upon the distance at which the measurement is taken, as illustrated in Fig. 10. In Fig. 9 and Fig. 10, the red line represents the ranging error of the original data, the black line represents the ranging error of the data after median filtering, and the green line represents the ranging error of the data after combined filtering.

As can be seen from Fig. 9, the raw data exhibits relatively poor measurement stability, whereas both median and combined filtering demonstrate

enhanced stability. The combined filtering method demonstrates the most optimal stability.

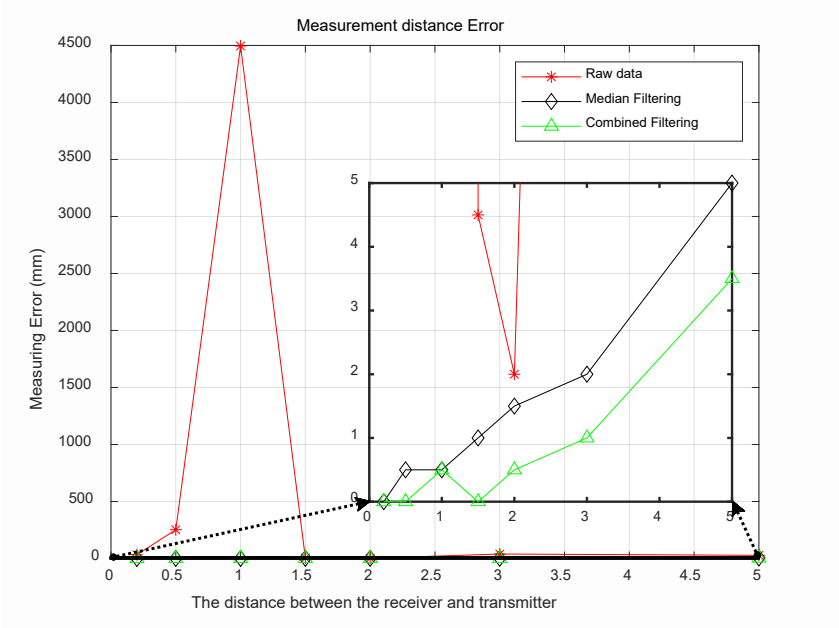

Fig. 10. Measurement Errors Corresponding to Different Distances

As it can be seen from Fig. 10, the measurement error due to the raw measurement data is quite large. The measurement error increases sharply due to the sudden interfering data and reaches an astonishing 4500mm when the distance is 1m. Since the median filter and the combined filter process the original data, the measurement errors are very small, and they are all less than ±1mm; when the measurement distance is within 3m, the measurement error of the median filter is less than ±2mm, and the measurement error of the combined filter is less than ±1mm. However, at a measurement distance of 5m, the measurement error gradually increases to ±5mm for the median filter and ±3.5mm for the combined filter.

6. Conclusions

This paper presents the working principle of a tracking ultrasonic sensor for distance measurement, designs the circuit for ultrasonic ranging, and introduces a combined filtering algorithm based on median filtering and Kalman filtering. The results of the testing indicate that the proposed method is capable of achieving high-precision measurements within a distance of 3 metres, with a measurement accuracy of ±1mm. This meets the requirements of most short-range distance measurement applications. However, at distances of 5 m, the

measurement error increases to ±3 mm. Given that the speed of sound is significantly influenced by environmental temperature and airflow and given that this system does not collect ambient temperature data, it is evident that further improvements are necessary for the system.

REFERENCES

[1] *Mirshahi, Shiva , and O. Mas*, A Novel Distance Measurement Approach Using Shape Matching in Narrow-Band Ultrasonic System, IFAC Symposium on Information Control Problems in Manufacturing, 2016.

[2] *Kevin Blümel, Flaviana Tagliaferri, Michael Kuhl*, Algorithm for calculating distance and sensor-object angle from raw data of ultra-low power, long-range ultrasonic time-of-flight range sensors, Procedia CIRP, 2023, pp.1061-1065.

[3] *Bischoff, O. , Heidmann, N. , Rust, J. , & Paul, S,* Design and Implementation of an Ultrasonic Localization System for Wireless Sensor Networks using Angle-of-Arrival and Distance Measurement. European Conference on Solid-State Transducers, 2012, pp. 953 – 956.

[4] *Rocchi A, Santecchia E, Barucca G, et al,* Optimization of distances measurement by an ultrasonic sensor, Materials Today: Proceedings, 2019, 19, pp. 33-39.

[5] *Licznerski T J, Jaroński J, Kosz D,* Ultrasonic system for accurate distance measurement in the air, Ultrasonics, 2011, 51(8), pp.960-965.

[6] *P. Hauptmann*, Application of ultrasonic sensors in the process industry, Meas. Sci. Technol, 13 R73, 2002.

[7] *M. Toa, A. Whitehead*, Ultrasonic Sensing Basics. revision d, Texas Instruments, 2021.

[8] *J.A. Ogilvy*, Theory of wave scattering from random rough surfaces, Bristol Institute of Physics, 1992.

[9] *Udomporn Manupibul, Ratikanlaya Tanthuwapathom, Wimonrat Jarumethitanont, Panya Kaimuk, Weerawat Limroongreungrat & Warakorn Charoensuk,* Integration of force and IMU sensors for developing low-cost portable gait measurement system in lower extremities, Scientific Reports, 13, 10653, 2023.